行政院國家科學委員會專題研究計畫　期中進度報告

薄膜機械特性及殘留應力之反算偵測(2/3)

計畫類別：個別型計畫
計畫編號：NSC92-2212-E-002-009-
執行期間：92 年 08 月 01 日至 93 年 07 月 31 日
執行單位：國立臺灣大學應用力學研究所

計畫主持人：吳恩柏

計畫參與人員：張家壽,邵清安

報告類型：精簡報告

處理方式：本計畫可公開查詢

中　華　民　國 93 年 5 月 24 日

行政院國科會專題研究計劃
薄膜機械特性及殘留應力之反算偵測 (2/3)
NSC 92-2212-E-002-009
執行期間：92 年 8 月 1 日至 93 年 7 月 31 日
計劃主持人：吳恩柏
執行單位：國立臺灣大學應用力學研究所
計劃參與人員： 張家壽、邵清安

摘要

隨著電子產品的微小化，許多光學量測技術紛紛朝著微小尺寸表面量測發展。本文成功結合數位投影疊紋法與立體顯微鏡，並運用相移及相位重建技術重繪出物體的三維表面輪廓。數位投影疊紋法不僅可直接用於大尺寸表面量測，並可將電腦製作出的近似正弦強度光柵，透過 DLP 投影機及透鏡組後導入至立體顯微鏡中，以用於小尺寸表面量測。此法可產生最小5μm間距微光柵，適用於50μm的微小尺寸範圍，可架構成為新式三維微小尺寸表面量測系統。由於投影疊紋法有所謂線性錯配法，且搭配相移技術及本實驗室發展的相位重建技術，可大大地增加疊紋數目而提高解析能力，並應用於薄膜機械特性及殘留應力之反算偵測。

關鍵字：數位投影疊紋法、立體顯微鏡、正弦強度光柵、DLP 投影機、相移、相位重建法、薄膜量測

ABSTRACT

With the rapid trend for miniaturization of electronic products, new optical techniques are increasingly needed for measuring the surface profile or deflection/warpage in the micro-scale for electronic packages mounted on printed circuit boards. In this paper, we have successfully reduced the grating spacing of the digital projection moiré (DPM) by directing the grating pattern into a stereo zoom microscope and performed surface profile measurement under this microscope. In this method, the reference grating is generated digitally having sinusoidal intensity. Another digitally generated grating is projected into the microscope to form the object grating. This is via a digital light processing (DLP) projector and a set of carefully arranged optical lens. The pitch of micro-scaled object gratings can be adjusted by the magnification of the microscope. As a result, this micro-scaled digital projection moiré method produces a 5-um pitch micro object grating and is suitable for surface profile measurement in a square dimension as small as 50-um. In order to obtain more fringes in each measurement, the method of linear mismatch is utilized and the guideline to achieve the optimal degree of linear mismatch between the reference and the object gratings is proposed. In addition, the phase shifting technique is employed to extract the data between the recorded fringes. These two procedures enhanced the measurement resolution to more than ten folds. Verification of the method is demonstrated by measuring the inclined plane of a micro prism. The deviation between the measured data and the given values is less than 5%. This method is then used to measure the profile of a solder ball on a flip chip package, thin film profile measurement.

Key Words: micro digital projection moiré, stereo zoom microscope, linear mismatch, phase shifting, surface profile measurement.

INTRODUCTION

Due to the tendency of continuous miniaturization of components in the semiconductor industry, specimen surface condition and residual stress influence the production quality significantly. Consequently, developing a three dimensional(3D) micro-scaled surface profile measurement system is very important. Among various full-field measurement methods, the projection moiré method is a good candidate as it does not require to install physical gratings on or above the object to be measured. In applying the projection moiré method to measure the surface profile of a millimeter scale field of vision, Huang et al.[1] utilized traditional digital fringe projection technique and the phase shifting technique to measure surface profile of 4mm size object. The surface profile was derived from the phase concept. Chung et al.[2] did similar work but the surface profile was derived from the concept of geometric optics. In their study, the grating pitch was limited because no microscope was employed. Further, the fringe number was also limited because no linear mismatch technique was used. In this paper, we directed the grating of the digital projection moiré(DPM) into a stereo zoom microscope to measure 3D surface profiles. The field of vision was as small as $50\mu m \times 50\mu m$. By implementing the linear mismatch technique, and the phase shifting algorithm , we are able to increase the spatial resolution up to 10 folds. The advantages of utilizing this method are non-contact, full field, real time and fast reaction. In section 1, we present the DPM principles and the experimental setup. In section 2, the DPM method is conducted to measure the slope of a micro prism and the surface profile of a solder ball in a flip chip package.

METHOD DEVELOPMENT

2.1 Digital Projection Moiré Method

To develop the digital projection moiré technique, we utilized the gratings generated by computer software and projected these gratings onto the object. We obtained the deformed object grating resulting from surface profile deformation, and then the object grating interfered with the reference grating to form the moiré pattern by computer software.

In this section, the near sinusoidal intensity grating generated by computer software is illustrated in Fig.1, which consist of 16 pixels in a period, that is, we utilized the gray level values of 16 pixels to describe the sinusoidal relationship.

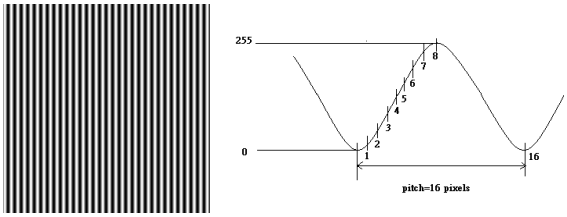

Fig.1 A sinusoidal intensity grating image, the period=16 pixel

After we recorded the reference grating data and object grating data, we evaluated four mathematic operation forms for extraction of optimal moiré patterns: 1. addition method: the gray level values of reference and object grating, in the forms of image matrices, were arithmetically averaged. 2. multiplication method: the two gray level values were multiplied and then square rooted. 3. subtraction and clip method: the two gray level values were subtracted, and the negative values

were taken as zero. 4. subtraction and taking absolute values: the two gray level values were subtracted by each other and the absolute value were obtained.

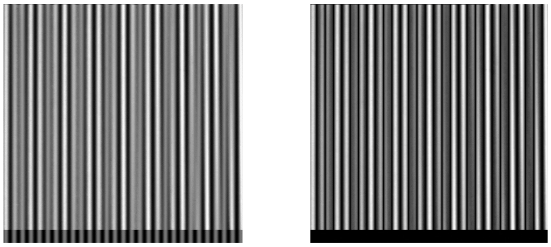

1. addition 2. multiplication

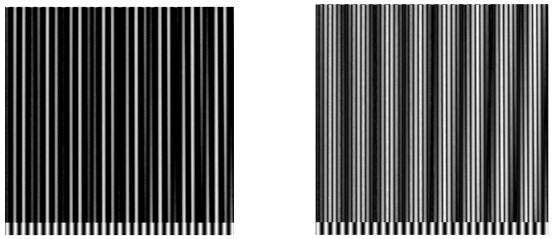

3. subtraction and clip 4. subtraction and taking the absolute value

Fig.2 Moiré pattern taken by four different mathematic operations

Fig.2 shows the example using the same reference and object gratings, but with the four mathematical operation mentioned above. Utilizing the fourth operation, we obtained the best contrast for the moiré pattern. So we adopted the operation by using subtraction and taking the absolute value.

The concept of digital projection moiré is as follows (Fig.3):

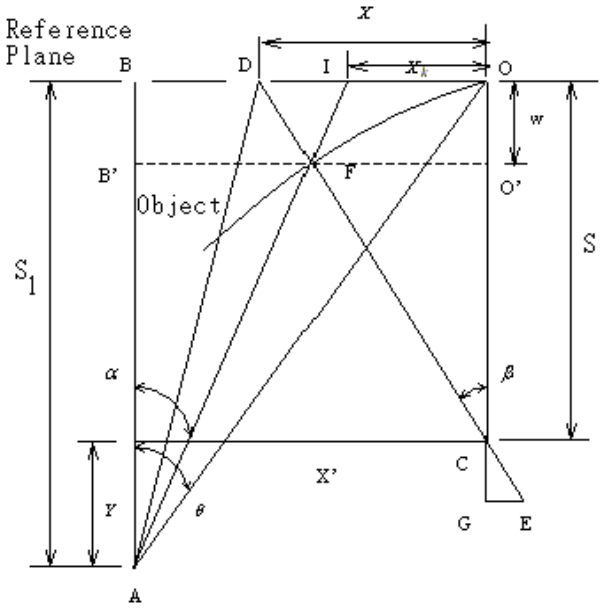

Fig.3 Digital projection moiré

In the most general case considered in the paper, the digitally generated grating is projected onto the object surface through a digital light processing(DLP) projector. The projected axis($\overline{AB}$) and the view axis($\overline{CO}$) are parallel to each other and both are perpendicular to the reference plane($\overline{BO}$) at the intersection point B and O. On the other hand, the projector (A) and the CCD(C) may not be on the same plane, it means that the axes of the projector and the CCD are parallel to each other, but the line($\overline{AC}$) from projector to CCD is not parallel to the reference plane. In this figure, O is the origin point on the reference plane, X spans half of CCD grab region, X_k spans half of view point region, S is the distance between the CCD and the reference plane, X' is the distance between the projector and the CCD, F is one view point of intersect, α is the projected angle, and β is the view angle. Giving, P_1 the pitch of the reference grating, P_2 the pitch of the object grating, in order to

enhance the spatial resolution, we let $P_1 \neq P_2$ to obtain the linear mismatch effect.

The moiré principle is

$$N = m_1 - m_2 = \frac{X}{P_1} - \frac{X_k}{P_2} \tag{1}$$

In Fig.3, by utilizing the geometrical optics method, we obtain a general expression of the out of plane warpage for the object to be measured

$$w = \frac{P_1P_2(S+Y)N + (S+Y)(P_1-P_2)X}{P_1P_2N + P_1(X'+XY) + (P_1-P_2)X} \frac{\sqrt{1+\frac{Z^2}{X^2+S^2}}}{\sqrt{1+\frac{Z^2}{S^2}}} \tag{2}$$

where Z is the location along the Z axis of the reference plane, which is pointed to Fig.3, and Y is the distance between the CCD and the projector.

In Fig.3, by letting the line connecting the projector to the CCD, $\overline{AC}$, be parallel to the reference plane, $\overline{BO}$, Eq.(2) is reduced to:

$$w = \frac{P_1P_2SN + S(P_1-P_2)X}{P_1P_2N + P_1X' + (P_1-P_2)X} \tag{3}$$

Note that Eqs.(2) and (3) are the projection moiré with point light source.

2.2 Micro-Digital Projection Moiré Method

If the light guided to the microscope is not in parallel, we need to determine many parameters and shown as Eq.(2) and (3). As a result, the system error can be drastically increased. On the other hand, if we incorporate a lens set in front of the DLP projector so as to produce parallel light, this parallel light can be guided into the stereo zoom microscope, as depicted Fig.4(a). In Fig.4(a) and (b), the CCD is perpendicular to the reference plane and its center intersects the parallel light at point $\overline{O}$, C is the CCD view point, $\overline{S}$ is the distance between CCD and reference plane, and $\overline{F}$ is a view point. When we define $\overline{O}$ as the reference point, $\overline{X}$ is the half of CCD grab region, and $\overline{X_k}$ is the distance between the intersection point $\overline{I}$ and point $\overline{O}$. As a result, Eq.(4) can be obtained by using Fig.4(b):

$$w = \frac{P_1P_2\overline{S}N + \overline{S}(P_1-P_2)\overline{X}}{P_1\overline{X}} \tag{4}$$

Thus, we only need to decide the reference grating pitch, the object grating pitch, the CCD grab region, and the distance between the CCD and the object in order to obtain the out-of-plane warpage w.

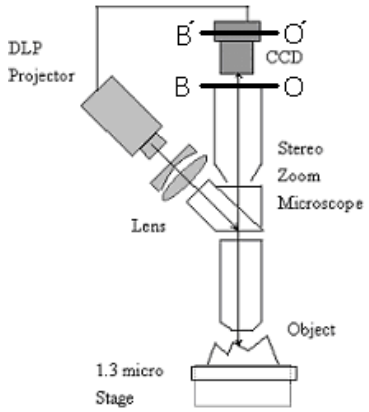

(a)

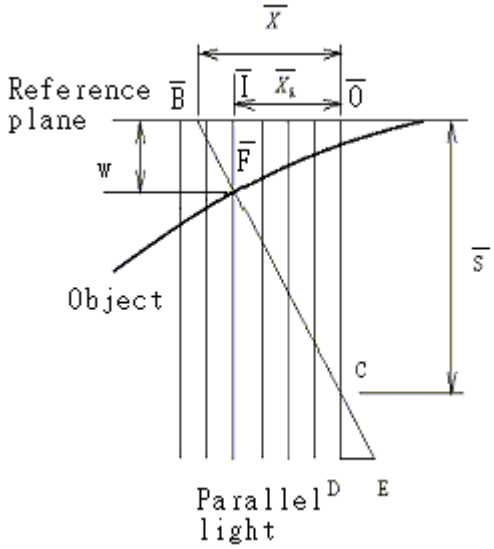

(b)

Fig.4 (a) Point light projected by DLP is converted into parallel light by the lens set. The light is then directed into the microscope, reflected by the object , and recorded by the CCD camera; (b) Parallel light generated from the projector, and reach CCD screen, $\overline{BO}$.

Further, in order to guide the parallel light from the stereo zoom microscope into the CCD, we install a TV adaptor, which also has a magnification factor, as show in Fig.5. As a result, the reference plane $\overline{BO} = \overline{X}$ is converted into $\overline{B'O'} = \overline{X'}$ and Eq(4) becomes

$$w = \frac{L'}{L}\frac{\overline{S}}{\overline{X}}\frac{P_1P_2N + (P_1 - P_2)\overline{X}}{P_1} \qquad (5)$$

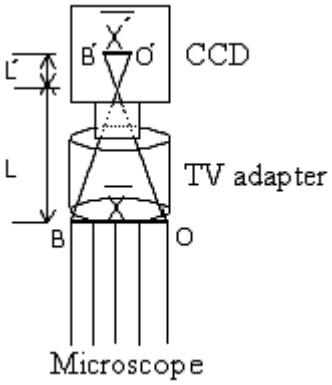

Fig.5 Grabbing the moiré image by a CCD from a stereo zoom microscope

where $\overline{S}$ is the distance between the CCD center to the reference plane, $\overline{X}$ is the grabbing range of a CCD on the reference plane. The ratio $\frac{\overline{S}}{\overline{X}}$ of Eq.(4) is converted into: $\frac{L'}{L}\frac{\overline{S}}{\overline{X}}$, cohere $\overline{S'}$ is the distance between the CCD center and the sensing area, and $\overline{X'}$ is the size of the sensing area.

2.3 Linear Mismatch Method

Once the moiré gratings are recorded, we then utilized the linear mismatch effect to determine the number of moiré fringes. The linear mismatch procedure is very important in the digital project moiré method, because it plays an important role on controlling the number of moiré fringes. Fig.6(a) shows moiré grating recorded from an inclined plane of 30^0 and Fig.6(b) is the average gray level distribution of this object grating image in the row direction. Point light source is employed in this case.

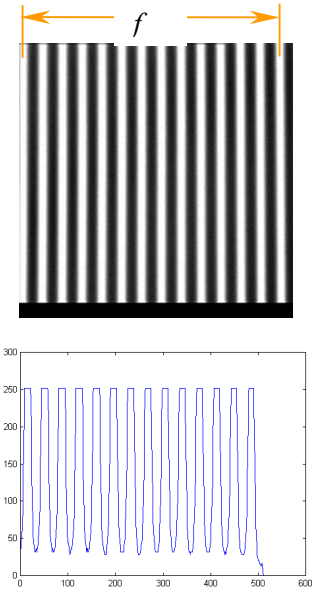

Fig.6 (a) The object grating picture of an inclined plane of 30^0; and (b) the averaged gray level distribution of the object grating image taken in the row direction

In Fig.6(b), we have known that the actual grabbing image range, X, and the image size of 512×512 pixel. So, we can find the pixel size, f, from the highest gray level of the first point to the highest gray level of the last point, and the grating number N in the range of f. By the proportional relationship, we can obtain the

actual grabbing image size x in range f. That is, we can obtain pitch P_2 of the object grating to be

$$x = f \times \frac{X}{512} \qquad P_2 = \frac{f}{N} \tag{6}$$

Using Fig.(6) as the object plane, we find thirteen fringes in the actual grabbing image size with 486 pixels, and it means 37.4 pixels per grating. Then we use 56、50、48、40、36、35、34、32、29、24、18、16 pixels per pitch for the reference grating. In order to study the linear mismatch effect, we need to define the difference pitch percentage(DPP) as

$$\left| \frac{object\ \ grating\ \ pitch - reference\ \ grating\ \ pitch}{object\ \ grating\ \ pitch} \right| \times 100\%$$

The result is listed in Table 1.

Pixel/pitch for Ref. grating	56	50	48	40	36	35	34	32	29	24	18	16
DPP (100%)	49.7	33.7	28.3	7.0	3.7	6.4	9.1	14.4	22.5	35.8	48.2	57.2
Fringe number	<6	<5	<5	<2	<1	<1	<1	<2	<4	<7	<14	no

Table 1. Effect of linear mismatch and its relationship to the number of moiré fringes for the gratings obtained from the object with inclined plane of 30^0

In Table 1, DPP increases with the number of the fringes increases. In general, it results in the linear mismatch effect when DPP value is low 50%. When DPP value is larger than 50%, the fringe contrast becomes indistinguishable. On the other hand, we tend to use smaller DPP in the case of parallel light, such as in the micro-scaled measurement. This is because in Eqs.(3) and (4), the term $P_1 - P_2$ is in both nominator and denominator whereas in Eq.(5), which is for the case of parallel light, the term $P_1 - P_2$ is in the nominator only. Consequently, the Eq.(5)'s linear mismatch effect in used Eq.(5) should be smaller than the linear mismatch effect if Eq(3) is used.

2.4 Phase Shift Algorithm

Before adopting the phase shift algorithm, we have to filter out the high frequency background noise. Fig.7(a) shows a projection moiré fringe obtained from the same object with 30^0 inclined angle, which also contains the background noise.

When the data are transformed into the Fourier domain, as shown in Fig.7(b), the low frequency peak corresponds to the fringe signal whereas the two higher frequency peaks are induced by the background noise. After these higher frequency noise peaks are filter out, a much more cleaner fringe pattern is obtained again by inverse Fourier transform method, as shown in Fig.7(c).

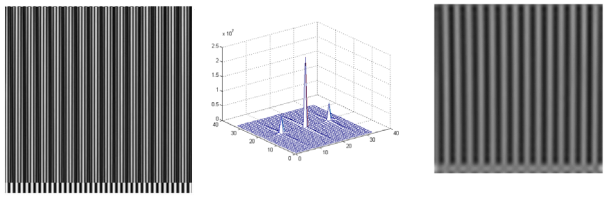

(a) (b) (c)

Fig.7 The moiré pattern via the Fourier transform and filter: (a) original data; (b) data in the Fourier domain; and (c) fringe picture after filtering.

The purpose of implementing the phase shifting algorithm is to increase the spatial resolution. In this paper, the four step method is adopted. Therefore, we need to shift the reference grating images four times, it means that every image matrix is shifted 4 pixels($=\pi/2$).

Because dusts inevitably exist on the surface of the object to be measured, the fringe

quality is always affected even after use of the aforementioned low-passed filtering process. Therefore, we adopted the branch cut algorithm for phase unwrapping[4]. The advantage of the branch cut algorithm is that it can bypass the localized zone that is contaminated by noises. Further, the unwrapping result is independent of the construction paths selected. Hence, the branch cut algorithm will greatly lower the noise propagation effect, and successfully rebuild the phase map.

After the unwrapped map is recorded, the rigid body rotation of the measured object surface is then removed by using the least square method[3]. Eq(5) is then employed to calculate the value of w . This completes the development of the micro digital projection moiré(MDPM) method.

3. EXPERIMENTAL RESULTS AND DISCUSSION

In this study, we choose the Digital light process(DLP) 350 projector by In focus, because it provides very high lumens and contrast, and is needed for obtaining high image quality. In addition, we use Sony XC-7500 CCD as the grabbing image system along with Nikon AF Micro-Nikkor 60mm f/2.8D lens. Besides, we use Nikon SMZ 2T stereo zoom microscope for micro-scaled measurement. The experimental setup is shown in Fig.8. We utilized Labview program to control a stepping motor to position and move the object to be measured under the microscope. The micro-scaled grating projects to the object is deformed with the surface profile of the object and is recorded by the CCD.

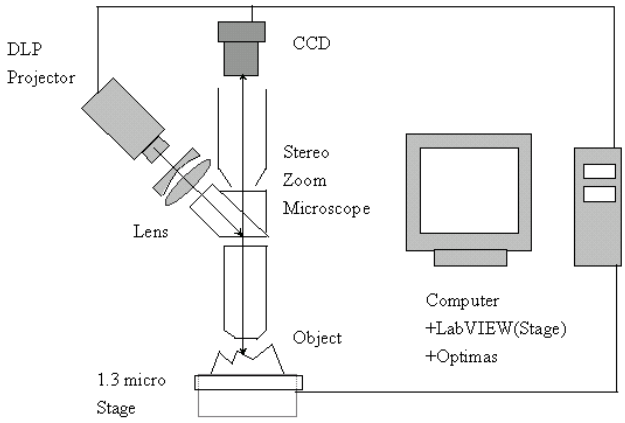

Fig.8 Experimental setup for micro-scaled surface profile measurement

The procedure described in Fig.8 is then employed to measure the surface profile of the object. To verify the developed method, we use a micro prism with dimension $1000(A)\times1000(B)\times300(C)\mu m$ as shown in Fig.9(a). Because the surface roughness is smaller than $1/4\lambda$,we assume the plane to have a smooth surface. A 20% linear mismatch is used in this example, and the field of vision of the CCD is $900\times900\mu m$. The filtered fringe recorded by the CCD mounted on the microscope is shown in Fig.9(b). The corresponding wrapped and unwrapped phase maps, and the 3D profile illustrated in Fig.9(c), (d), and (e), respectively.

C

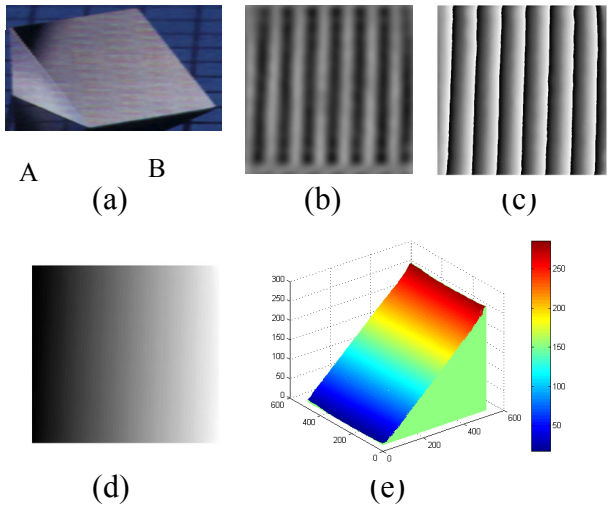

Fig.9 A micro prism used for micro-scaled surface profile measurement. (a) prism picture; (b) filtered fringe; (c) phase map; (d) unwrapped phase map; (e) 3D profile

Fig.10 is a comparison between the measured data and the actual profile of the micro prism. The data are taken from 255th pixel in the x-direction. Which is at the middle of the plane shown in Fig.10(e). The deviation between the measured data and the actual profile values is listed in Table 2. The satisfactory correlation verifies the method developed in this paper.

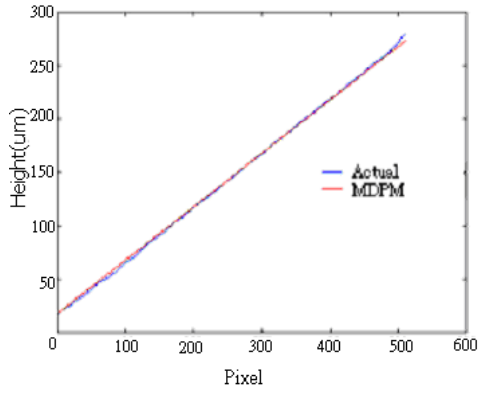

Fig.10 Comparison of the results recorded by the developed MDPM method and the surface profile of the micro prism

Location(y-pixel)	100	200	300	400	500
MDPM(μm)	68	121	170	224	271
Actual(μm)	70	122	169	220	285
Deviation(100%)	-3.0	-1.0	1.0	2.0	4.9

Table 2 Comparison between the MDPM method and the actual surface profile of the micro prism, the measured locations are along the y-direction in Fig.9(e)

We then use the MDPM method to measure a solder ball on a flip chip package. The level of linear mismatch is 15% in this example because the profile is more drastically changed comparing to the prism used in Fig.10. The field of vision used is also $900\times900\mu m$. The ball diameter is approximately 650 μm, as shown Fig.11(a). The magnified solder ball and the object grating, the unwrapped phase diagram of the solder ball, and its 3D surface profile are illustrated in Fig.11(b), (c) and (d), respectively.

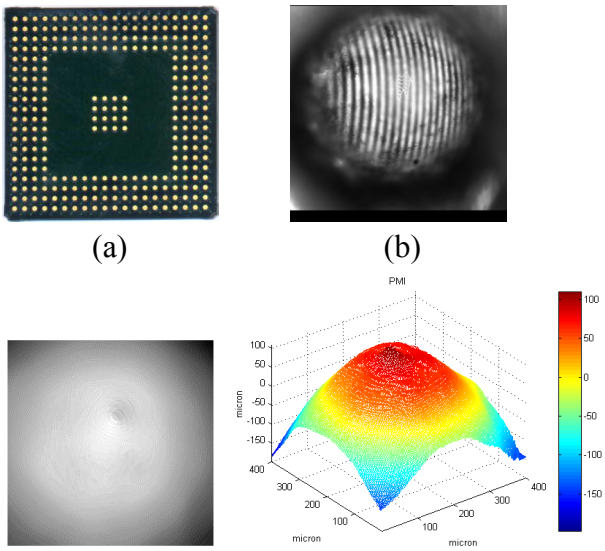

Fig.11 Flip chip solder ball surface profile measurement by MDPM method: (a) a flip chip package; (b) magnified solder ball and the object grating; (c) unwrapped phase map; and (d) the corresponding 3D surface profile.

The range of the field of vision is determined by the focal length and the TV adaptor of the microscope used. In this study, the smallest field of vision reached is $50\times50\mu m$ due to the limitation of the hardware. On the other hand, the grating pitch is determined by the originally grating generated by the computer, the magnification of the micro scale, and the resolution of the CCD used. Fig.12 illustrates two examples both of which have a field of vision of $50\times50\mu m$. In Fig.12(a), the grating

pitch is $10\mu m$, which is produced using 8 pixel per grating. On the other hand, 4 pixel per grating is used in Fig.12(b), which results in $5\mu m$ grating pitch.

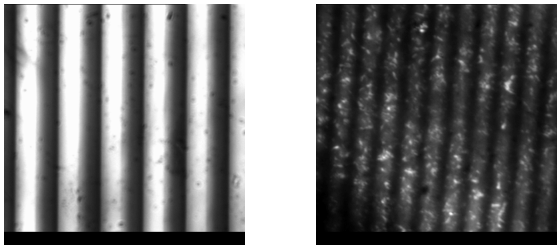

(a) (b)

Fig.12 The object grating in a square dimension as small as 50-um, (a) $10\mu m$ pitch; and (b) $5\mu m$ pitch

CONCLUSIONS

In this paper, we first developed a digital projection moiré technique by adopting the geometrical optics concept and obtain a general expression for the surface profile measurement of an object. Then, we combined a stereo zoom microscope and the developed digital projection moiré technique to obtain a new measurement technique designated as the micro-digital projection moiré (MDPM) method, MDPM is suitable for micro-scaled surface profile measurement. The measurement range is from mm scale to $50\mu m$, and the grating pitch is as small as $5\mu m$. In this method, the linear mismatch effect is utilized increase the fringe number, and the phase shift algorithm is adopted to enhance the spatial resolution of the phase map. We did the verification runs for both the larger scale and micro-scaled components, which demonstrated the validity and versatility of the developed MDPM.

ACKNOWLEDGMENTS

This research is supported by National Science Council of Taiwan, ROC, under contract number NSC92-2212-E-002-009.

REFERENCES

1. P. S. Huang, F. Jin, F. P. Chiang, "Quantitative Evaluation of Corrosion by A Digital Fringe Projection Technique," *Optics and Lasers in Engineering*, Vol.31, pp.371-380, 1999.
2. D. E. Chung, C. A. Shao, T. C. Hsu, "The Theory and Application of Flatting and Shape Measurement in Electronic Scanning Moiré Method," *Department of Mechanical Engineering, Yuan Ze University*, Master Thesis 1999, (in Chinese).
3. I. T. Tsai, C. A. Shao, E. Wu, "The Application of Phase-Evaluation Methods and Image Processing on Electronic Packages," *Institute of Applied Mechanics, National Taiwan University*, Master Thesis 2000, (in Chinese).
4. J. R. Buckland, J. M. Huntley and S. R. E. Turner, "Unwrapping Nosy Phase Maps by Use of a Minimum-cost-matching Algorithm", *Applied Optics*, Vol.34, pp.5100-5108, 1995.